Simulation of Image Detail Visibility using Contrast Sensitivity Functions and Wavelets

Marius Pedersen and Ivar Farup.

**** The Norwegian Colour and Visual Computing Laboratory, Gjøvik University College (Norway).***

Abstract

Natural images contain a lot of information imperceptible to the human eye. While it is of key importance to maintain the visible information in image reproduction processes, the imperceptible information can, with good benefit, be discarded. In order to identify the imperceptible information, a method for simulating this particluar aspect of the human visual system is required. In this paper we present a robust contrast filtering method for simulating the detail visibility of natural images. The method removes image spatial-frequency components that are undetectable at a given viewing distance. The method is based on the relationship between contrast sensitivity and spatial frequency (contrast sensitivity functions) and octave-wise spread over the spatial frequency range matched by wavelet decompositions. An experimental evaluation of the method, where simulated distance is compared to observered discrimination distance, shows promising results. The proposed contrast filtering method has a wide range of applications; it can be used in, e.g., image quality metrics, image compression, gamut mapping, and halftoning.

Introduction

Natural images contain a lot of information that is imperceptible to the human eye. In many cases the imperceptible information is unwanted, for example in compression where the imperceptible information can be compressed more, or even completly removed, compared to perceptible information while maintaining quality [1]. Imperceptible information should not be included in the image quality evaluation [2], in gamut mapping perceptible and imperceptible information can improve the quality of the image [3], while in halftoning it can be used to maximize image quality [4]. In order to ensure that only the imperceptible information is filtered from the image, a robust and powerful method of this particular aspect of the human color vision is required.

Typically, methods simulating the Human Visual System (HVS) account for a number of psychophysical effects, usually implemented in a sequence of processes. The first stage is to transform the image into a suitable perceptual color space, most likely an opponent-color space. In the next stage, since the HVS bases its perception on multiple channels that are tuned to different spatial frequencies and orientations, the image is decomposed into multiple channels. Next, local contrast estimation and adaptation is carried out. The next stage deals with one of the important issues, the decreasing sensitivity for higher spatial frequencies. This is characterized by the Contrast Sensitivity Function (CSF). A common last process is to account for masking, i.e. when a stimulus that is visible by itself cannot be detected due to the presence of another.

Several methods simulating the HVS have been proposed, some are based on CSFs used to modulate frequencies that are less perceptible [5]. The common way to do this is to use convolution kernels to "blur" the spatial frequencies that observers cannot perceive [2]. Many specify and implement the CSFs in the frequency domain [6]. Many of the methods simulating the HVS are linear processes that ignore the highly nonlinear characteristics of the HVS [7]. A robust nonlinear method is therefore required to simulate the detail visibility of images point by point and for every spatial frequency in the image. Such a method has great potential, it can among others be used for measuring image quality, optimization of quality, in design, and simulation of image appearance.

This paper focuses on developing a robust and powerful method to simulate the detail visibility of images according to the HVS. With this in mind the paper is organized as follows; first an introduction to relevant background, before we propose a new filtering method based on CSFs and wavelets, then an evaluation of the proposed method. We continue with showing how the method can be incorporated in an image quality metric to improve quality evaluation. At last, we conclude and propose future work.

Background

Peli [7] introduced a method to simulate the HVS, where contrast at each point in an image is calculated separately to account for variations across the image, and since contrast sensitivity depends on frequency, contrast is also calculated for different frequency bands. Peli [7] proposes the idea of a pyramidal image-contrast structure where for each frequency band, the contrast is defined as the ratio of the bandpass-filtered image at that frequency to the lowpass image filtered to an octave below the same frequency (local luminance mean).

To define local band-limited contrast for a complex image, he obtains a band-limited version of the image in the frequency domain $A(u,v)$:

$$A(u,v) \equiv A(r,\theta) \equiv F(r,\theta)G(r), \tag{1}$$

where u and v are the respective horizontal and vertical spatial frequency coordinates, $G(r)$ is a band-pass filter, and r and θ represent the respective polar spatial frequency coordinates: $r = \sqrt{u^2 + v^2}$, $\theta = \tan^{-1}(u/v)$, and $F(r,\theta)$ is the Fourier transform of the image $I(x,y)$ in polar coordinates.

In the spatial domain the filtered image $a(x,y)$ can be represented similarly, that is, as:

$$a(x,y) = I(x,y) * g(x,y), \tag{2}$$

where $*$ is the convolution, and $g(x,y)$ is the inverse Fourier transform of the band-pass filter $G(r)$. In Peli's approach of measuring local contrast, the pyramid is obtained as follows:

$$A_i(u,v) \equiv A_i(r,\theta) \equiv F(r,\theta)G_i(r), \tag{3}$$

where $G_i(r)$ is a cosine log filter centered at frequency of 2^i cycles/picture, expressed as:

$$G_i(r) = \frac{1}{2}\left(1 + \cos\left(\pi \log_2 r - \pi i\right)\right). \tag{4}$$

The resulting contrast at the band of spatial frequencies can be represented as a two-dimensional array $c_i(x,y)$:

$$c_i(x,y) = \frac{a_i(x,y)}{l_i(x,y)}, \tag{5}$$

where $a_i(x,y)$ is the corresponding local luminance mean image and $l_i(x,y)$ is a low-pass-filtered version of the image containing all energy below the band. This filtering differs from other types of filtering because suprathreshold features retain contrast and are not washed out [7].

Pedersen et al. [8] extended the the contrast filtering by Peli [7] to chromatic information. First the image is transformed into the CIEXYZ color space. However, since the CIEXYZ color space is not orthogonal, the channels were separated into a color part and a luminance part. To obtain the luminance bandpass information in the color channel (X_{BL}), the lowpass information in the color channel (X_L) is divided by the lowpass information in the luminance channel (Y_L), and further multiplied with the bandpass information in the luminance channel (Y_B): $X_{BL} = (X_L/Y_L)Y_B$. Having separated the color and luminance information, for each channel independently, the contrast of every pixel is calculated as described in Equation 5. The contrast c is compared against the contrast sensitivity threshold for the corresponding channel for each band. If the contrast is suprathreshold the information is perceptible and kept, and if the contrast is subthreshold the information is discarded. The filtering by Pedersen et al. [8] was used in an image quality metric, Total Variation of Difference (TVD). TVD showed promising results compared to other metrics.

Nadenau et al. [1] proposed a wavelet-based color image compression technique that exploited the CSF. Wavelets have the advantage over DCT approaches that they significantly improves quality at lower bitrates. Additionally, from psychophysical experiments it has been shown that our HVS works with octave-wise spreads over the spatial frequency range, that match the structure of wavelet decompositions [9]. Wavelets also allow for higher spatial resolution at the highest frequencies. Nadenau et al. [1] decomposes the image with a wavelet, and for each level a subband-specific filter of horizontal and vertical spatial frequencies are computed. First the sampling frequency f_S in pixels per degree is found:

$$f_S = \frac{2v\tan(0.5^\circ)r}{0.0254}, \tag{6}$$

where v is the distance in meters, r the resolution measured in pixels per inch. If the signal is downsampled at Nyquist rate, 0.5 cycles per pixel are obtained. This gives a maximum frequency of:

$$f_{max} = 0.5 f_S. \tag{7}$$

For implementation of the CSF Nadenau et al. [1] suggest four different approaches, from a simple invariant weighting factor per subband to more advanced methods using Finite Impulse Response (FIR) filters.

Proposed method

We propose a new contrast filtering method for the simulation of image detail visibility based on the work of Peli [7], Nadenau [1, 10], and Pedersen et al. [8]. The basis of most HVS filtering methods are CSFs, where the sensitivity to luminance and two opponent color channels (red-green and blue-yellow) are measured [11]. Using these CSFs require a color space matching the conditions of the experiments in which the CSFs were measured, namely a color space with a luminance and two opponent channels. Nadenau and Reichel [10] previously showed that the color space in which the filtering is performed is important, and care should be taken to select the most appropriate color space. They found the YC_bC_r color space to be the most approriate.

For proposed contrast filtering method we present a new linear color space inspired by the YC_bC_r color space. We assume a sRGB input image, which is linearized to remove the gamma correction, the linear RGB image is transformed into CIEXYZ, and then further into a new RGB space. The primaries of the new RGB space are defined according to the wavelengths of the gratings used in the experiments by Mullen [11] to measure the chromatic CSFs, where red is 602 nm, green 526 nm, and blue 470 nm. Since the gratings are monochromatic, the transformation from CIEXYZ to the new RGB color space is straightforward. Further, the image is transformed into a our new color space Ybr:

$$Y = Y_r R + Y_g G + Y_b B, \tag{8}$$

where R, G, and B are the new linear RGB values, Y_r, Y_g, and Y_b are the $\bar{y}$ values from the color-matching functions for the red, green, and blue channels, such that Y is the CIE luminance. The color channels are defined as:

$$b = \frac{Y_b B}{Y}, \tag{9}$$

and

$$r = \frac{Y_r R}{Y}. \tag{10}$$

In this new linear Ybr color space, the channel contrasts correspond exactly to the contrast definitions used by Mullen [11]. Thus their curves can be applied directly. Also, the channels are decorrelated such that pure luminance contasts only appear in the Y channel, and pure chrominance contrasts only appear in the b and r channels. This is clear advantage over using the CIEXYZ color space as done by Pedersen et al. [8].

After the color transformations the filtering according to the HVS can be performed. We base the new method on existing work on local band-limited contrast for complex images by Peli [7] and the wavelet based contrast sensitivity filtering by Nadenau et al. [1].

The image is transformed into the new Ybr color space, and then a wavelet decomposition is carried out to obtain a octave width bands of frequencies. At the lowest level the coefficients of the low-pass filtered version (approximation coefficients) are reconstructured to fullscale (LL). The three high-passed filtered versions (detail coefficients), containing three orientations (ψ); horizontal, vertical, and diagonal (HL, LH, and HH) are extracted. These are also reconstructed to fullscale, before they are filtered with the CSFs, becoming the filtered image a. By appyling the CSFs to fullscale reconstructed coefficients we reduce artifacts when thresholding. Furthermore, the application of the filter is straightforward since we do not need to "mirror" or scale the CSFs as done by Nadenau et al. [1]. For the achromatic channel (Y) a luminance CSF is applied, and for the two chromatic channels (b and r) chromatic CSFs are applied.

For making the proposed filtering method more robust, an achromatic CSF accounting for the luminance level is advantageous. Therefore, we adopt the CSF from Barten [12], which gives the proposed method greater flexibility:

$$CSF_L = \alpha f \exp(-\beta f)\sqrt{1+\gamma\exp(\beta f)}, \tag{11}$$

where

$$\alpha = \frac{540(1+0.7/\lambda L)^{-0.2}}{1+\frac{12}{w(2+u/\gamma)^2}}, \tag{12}$$

$$\beta = 0.3(1+\frac{100}{\lambda L})^{0.15}, \tag{13}$$

$$\gamma = 0.06, \tag{14}$$

L is the effective display luminance in candelas per square meter, f is cycles per degree, w is the angular display size in degrees, λ is a brightness-reduction compensation factor [13] defined as $0.187 + 0.355e^{-10^{-5}E/0.073}$ for illuminance $E \geq 162$ and $1-(287.67E)./(10^5)$ for illuminance $E < 162$.

For the chromatic content, two CSFs are required, one for the red-green channel and one for the blue-yellow channel. Less work has been carried out when it comes to chromatic CSFs, and most well-known work is from Mullen [11], van der Horst and Bouman [14], and Poirson and Wandell [15]. Johnson and Fairchild [6] found that the sum of two Gaussian functions fitted the previous works well, and proposed the following chrominance CSF:

$$CSF_C = \alpha_1 e^{-\beta_1 f^{\gamma_1}} + \alpha_2 e^{-\beta_2 f^{\gamma_2}}, \tag{15}$$

where the parameters for the red-green and blue-yellow channels are given by Table 1, and f is defined as cycles per degree.

Table 1: Parameters for the chrominance CSFs.

Parameter	red-green channel	blue-yellow channel
α_1	109.14130	7.032845
β_1	-0.00038	-0.000004
γ_1	3.42436	4.258205
α_2	93.59711	40.690950
β_2	-0.00367	-0.103909
γ_2	2.16771	1.648658

The luminance CSF (CSF_L) is applied to the luminance channel, and the chrominance CSFs (CSF_C) are applied to the chrominance channel for each band and orientation. It should be noted that the CSF functions are not normalized and applied directly at the given scale.

Now, let $l'_j(x,y)$ denote the contrast filtered LL band and $h_{\psi j}$ denote the HL, LH, and HH bands (depending on ψ) at level j. At the lowest level, the LL band is not filtered, thus $l'_N(x,y) = l_N(x,y)$, where N denotes the lowest level. Further, let $a_{\psi j}(x,y)$ denote the CSF filtered version of $h_{\psi j}(x,y)$ as described above. Then, the contrast filtered octave bands are defined as

$$h'_{\psi j}(x,y) = \begin{cases} h_{\psi j}(x,y) & \text{if } a_{\psi j}(x,y) > l'_j(x,y) \\ 0 & \text{else} \end{cases} \tag{16}$$

The filtered information in the three orientations are then summed and added to the low-pass filted version to obtain the low-pass filtered version for the next level:

$$l'_{j+1}(x,y) = l'_j(x,y) + \sum_{\psi=1}^{3} h'_{\psi j}(x,y). \tag{17}$$

Although our HVS can be described by different frequency bands, they are not strictly band-limited and interection between the bands can occur [16]. Several effects are often discussed in the literature; the summation effect, contrast masking effect, and luminance adaptation. The first refer to an inter-channel effect where neighbouring frequency channels influence the total contrast, resulting in a sub-threshold response giving a response if there exists excitory stimuli nearby. However, this effect has been shown to be less important than contrast masking [17], and is therefore not accounted for in this work. The masking effect is when the visibility of stimulus at some frequency is impaired by the presence of another stimuli in a nearby frequency. This can be seen as a reduction in contrast sensitivity threshold a certain frequency in a specific region [16]. Luminance masking refers to the effect when sensitivity to intensity differences is dependent on the local luminance in regions [18].

A common way to account for luminance adaptation is to divide the energy in a frequency band by an estimate of the local lowpass filtered luminance version of the image [18]. This effect is already accounted for in Peli's approach, since the energy in a frequency band is divided by an estimate of local luminance [18].

Contrast masking is difficult to account for, mainly since masking is highly dependent on the masker and target stimulus, but also since masking in an image will depend on the familarity of the image to the observer [18]. The lack of contrast masking is thought to be a significant reason why many image quality metrics are not correlated with perceived quality [18]. Contrast masking results in two effects: positive masking and negative masking. The negative masking, also known as the pedestal effect, is when the masker facilitate signal detection. Legge and Foley [19] showed that the pedestal effect greatly diminished when the masker and signal differ by ± 0.5 octaves, which makes it difficult to incorporate when simulating the detail visibility of one image. We therefore focus on the most important masking; positive masking.

Nadenau [20] proposed two different intra channel masking models, one simple model and an extended model accounting for local activity. Ninassi et al. [21] showed that masking models with a performing semi-local masking performed better than those without. Therefore, we apply the extended model from Nadenau [20]. This model is approximated by two piece-wise function with an inhibitory term that takes into account the neighbourhood activity:

$$T_{l,o}(m,n) = \max(1, \tilde{c}_{l,o}(m,n)^{\epsilon}) \cdot (1 + \omega_{\rho}), \tag{18}$$

where T is the threshold elevation, $\tilde{c}_{l,o}(m,n)$ is the wavelet coefficients normalized by the CSF for a given subband l and orientation o at pixel location (m,n), ϵ is the slope-parameter, ω_{ρ} is the correction term for the influence of an active or homogeneous neighbourhood:

$$\omega_{\rho} = \frac{1}{(k_L)^{\vartheta} N_{\rho}} \sum_{\rho} |c\tilde{}_{l,o}|^{\vartheta}, \tag{19}$$

where k_L determines thes dynamic range of ω_{ρ}, N_r specifies the number of coefficients in the neighbourhood ρ (here used an n-by-n neighbourhood), and ϑ is the power. We have followed the recommendation by Nadenau [20] regarding the parameters ($N_{\rho} = 84$, $k_L = 10^{-4}$, and $\vartheta = 0.2$), the slope-parameter is set to 0.62 as suggested by Legge and Foley [19], with a 3×3 neighbourhood. Masking is performed within each color channel, between orientations, and between levels.

There are various wavelet filters available with different properties. The choice of the optimal wavelets must be based upon several criteria, such as support size, number of vanishing moments, symmetry, smoothness, and orthogonality and biorthogonality [22]. Also, the order of the wavelet could potentially influence the filtering, as well as the number of decomposition levels. Evidence has been found that the choice of wavelets should be adjusted to image content and the application [23, 24].

The luminance CSF has a bandpass shape, and has a maximum around 4 cycles per degree. When using the proposed filtering for optimization of quality with a bandpass luminance CSF it could occur that information below the maximum is filtered, and then later the image is viewed further away, for example where we are most sensitive, then information that has been removed would be visible. To avoid this, the luminance CSF needs to be kept constant for frequencies below the maximum sensitivity [1, 18].

Evaluation of the proposed method

Since the proposed method should reflect the HVS, evaluation of the proposed method is required to ensure correspondence with visual observations. The method was tested by presenting the original image and the filtered image from a certain distance, if the method is valid, the filtered image and the original should be indistinguishable from a distance equal to or farther than the distance assumed in the filtered image [25]. The images should be progressively easier to distinguish when the distance is shorter than the simulated distance.

Experimental Setup

A total of 15 obervers, who all passed a visual acuity test, were shown two images at the time, one original and one filtered image. The observers indicated which of the two images appeared blurrier. The images were shown on a Dell 2407WFPb monitor, calibrated to sRGB. The monitor luminance was set to 80 cd/m2, according to the sRGB specification. In total, three different scenes were presented to the observers (Figure 1). The images had red–green, blue–yellow, and achromatic areas. The images were approximately 450 by 450 pixels. For each of the images two distances were simulated, four and two meters, using Symlets (sym15) with five decomposition levels. The observers started to view the images at a distance larger than the simulated distance, where each image at each simulation distance was presented two times at each viewing distance, and the observers were instructured to indicate which image that was blurred. Then the observers moved closer to the monitor, repeating the process. In images where the observers could not discriminate the filtered image, they were allowed to guess or skip to the next image (counting as not being able to discriminate the images).

(a) Image 1: Cam (b) Image 2: Fish (c) Image 3: Rock

Figure 1. *Test images used in the evaluation of the proposed method.*

Data analysis

From each distance the percentage of correct identifications of the simulated image was calculated for the three different images. The distance at which the subjects obtained a 75% correlated identification was compared with the simulated distance [25]. If the proposed method match the perception correctly, the measured and simulated distance should be equal.

Results

Results for the simulated distances are shown in Figure 2. From the plots it can, in general, be identified that the 75% discrimination threshold is at a slightly shorter distance than the simulated distance. In total for the three scenes simulated at 4 meters, a 66% discrimination is found at 4 meters and 77% at 3.5 meters. For the simulated 2 meters (Figure 2(b)) a 54% discrimination is found at 2 meters and 79% at 1.5 meters, indicating that the 75% threshold is just above 1.5 meters. However, for both the simulated distances at 4 and 2 meters some individual differences among the images are found, e.g. the fish image seems to be the hardest to discriminate. Additional experiments are required to determine whether this is is due to the dominant blue–yellow color, the structural content or other reasons. The results here indicate that with the current CSFs that the method does not filter enough information, and that more aggressive CSFs could be applied. However, in a setting where the method is used for optimization of quality (for example image compression) it is preferable that the method filters less rather more information in order to avoid visible artifacts.

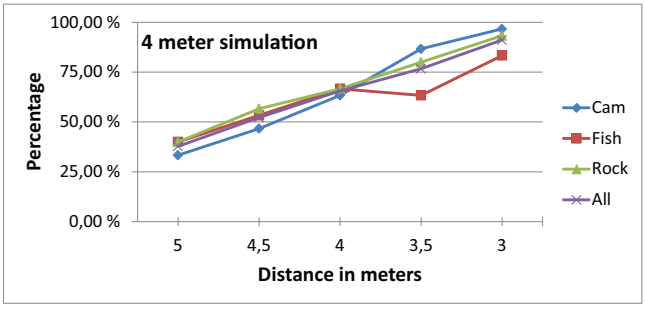

(a) 4 meters simulated.

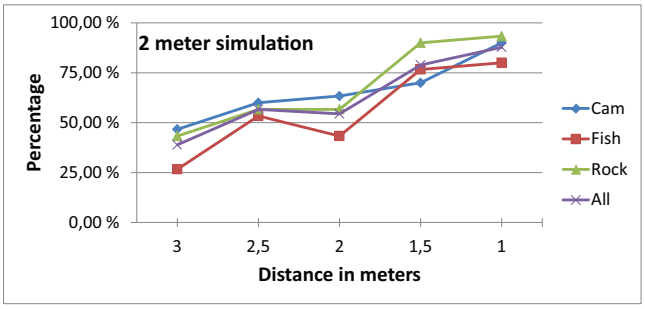

(b) 2 meters simulated.

Figure 2. *Evaluation of the proposed method. The method were evaluated at two different distances by 15 observers.*

Application of the proposed method

The proposed contrast filtering method has several different application areas, such as image quality metrics, gamut mapping, halftoning, deblurring. We show an example how the new contrast filtering method can be applied to image quality metrics. It has been shown that metrics incorporating features of the HVS are more robust than those who do not [26]. To demonstrate the new filtering method we will use the TVD metric [8]. We have calculated the results using the TVD with the new filtering and the standard filtering from S-CIELAB [2], which is based on convolution kernels to blur the image according to CSFs. Further, we calculate the correlation coefficients between the results from the metrics to observer scores.

A quality database is required to evaluate the performance of the metric with the new filtering. Large existing databases, such as LIVE [27] and TID [28], do not have a specified viewing distance, making them unsuitable. Therefore, we have used the dataset from Ajagamelle et al. [29], containing ten original images with eight different changes in contrast, lightness, and saturation (80 images in total). 14 observers judged the perceived difference between the original and the reproductions from a distance of 70 cm, forming the basis for the observer scores. As a performance indicator the linear Pearson correlation between the metric scores and observer quality scores (z-scores) has been calculated for each original image.

The results from the evaluation are shown in Figure 3. From the correlation plot we can see that TVD with the new filtering method has higher correlation than TVD with S-CIELAB filtering in 9 of the 10 images. In six of the images the correlation of the proposed filtering is more than 0.14 higher than the S-CIELAB filtering. A paired T-test shows that the proposed method is significantly better than with the S-CIELAB filtering (p-value of 0.019), and a sign-test shows the same result (p-value of 0.021).

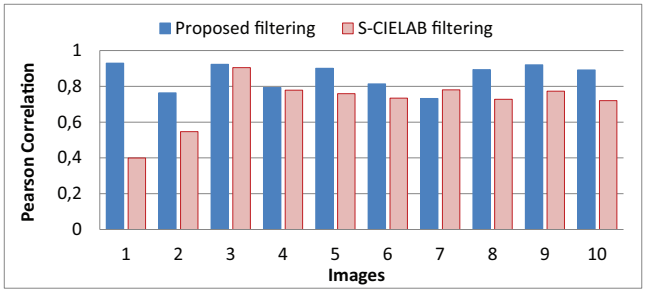

Figure 3. *Correlation between TVD metric, with the proposed filtering and with S-CIELAB filtering, and observer scores. In 9 of 10 images the TVD with the proposed has higher correlation coefficients than TVD with S-CIELAB filtering.*

Conclusion

In this paper we have proposed a new method for simluation of image detail visibility according to the contrast sensitivity function. The method performs the filtering in a specifically designed color space by using wavelets. Evaluation of the novel method showed promising results. At last we incorporated the new contrast filtering method in an image quality metric, showing that the performance of the metric increased compared to a standard filtering method.

Future work will include incorporation of additional aspects of the human visual system, and investigation of the possibilites of incorporating the proposed method into an image appearance model. We will also perform additional evaluation of the method, as well as how it can be used in different applications.

References

[1] M.J. Nadenau, J. Reichel, and M. Kunt. Wavelet-based color image compression: exploiting the contrast sensitivity function. *IEEE Transactions on Image Processing*, 12(1):58–70, jan 2003.

[2] X. Zhang and B. A. Wandell. A spatial extension of CIELAB for digital color image reproduction. In *Soc. Inform. Display 96 Digest*, pages 731–734, San Diego,CA, 1996.

[3] S. Nakauchi, S. Hatanaka, and S. Usui. Color gamut mapping based on a perceptual image difference measure. *Color Research and Application*, 24:280 –291, 1999.

[4] T. N. Pappas, J. P. Allebach, and D. L. Neuhoff. Model-Based Digital Halftoning. *IEEE Signal Processing Magazine*, 20(4):14–27, July 2003.

[5] G. M. Johnson and M. D. Fairchild. On contrast sensitivity in an image difference model. In *Image Processing, Image Quality, Image Capture, Systems Conference (PICS)*, pages 18–23, Portland, OR, Apr 2002.

[6] G. M. Johnson and M. D. Fairchild. Darwinism of color image difference models. In *Color Imaging Conference*, pages 108–112, Scottsdale, AZ, Nov 2001.

[7] E. Peli. Contrast in complex images. *J. Opt. Soc. Am. A*, 7:2032–2040, 1990.

[8] M. Pedersen, G. Simone, M. Gong, and I. Farup. A total variation based color image quality metric with perceptual contrast filtering. In *International conference on Pervasive Computing, Signal Processing and Applications*, Gjøvik, Norway, Sep 2011.

[9] M. A. Garcia-Perez. The perceived image: Efficient modelling of visual inhomogeneity. *Spatial Vision*, 6 (2):89–99, 1992.

[10] M. J. Nadenau and J. Reichel. Opponent color, human vision and wavelets for image compression. In *Color Imaging Conference*, pages 237–242, Scottsdale, AZ, Nov 1999.

[11] K. T. Mullen. The contrast sensitivity of human colour vision to red-green and blue-yellow chromatic gratings. *The Journal of Physiology*, 359:381–400, 1985.

[12] P. G. J. Barten. *Contrast sensitivity of the human eye and its effect on image quality*, chapter 3, pages 25–64. HV Press, 1999.

[13] S. Westland. Assessment of image difference and image quality. In *CREATE*, Bristol, UK, Sep 2007. 07/09/12: `www.create.uwe.ac.uk/Sep07_talks/Westland.pdf`.

[14] G. J. C. van der Horst and M. A. Bouman. Spatiotemporal Chromaticity Discrimination. *J. Opt. Soc. Am. A*, 59:1482–1488, Nov 1969.

[15] A. B. Poirson and B. A. Wandell. Appearance of colored patterns: pattern-color separability. *J. Opt. Soc. Am. A*, 10(12):2458–2470, 1993.

[16] Y-K. Lai. *Perceptual image quality measurement and coding with wavelets*. PhD thesis, University of Southern California, 1998.

[17] G. C. Phillips and H. R. Wilson. Orientation bandwidths of spatial mechanisms measured by masking. *J. Opt. Soc. Am. A*, 1(2):226–232, Feb 1984.

[18] M. P. Eckert and A. P. Bradley. Perceptual quality metrics applied to still image compression. *Signal Process.*, 70(3):177–200, 1998. doi: http://dx.doi.org/10.1016/S0165-1684(98)00124-8.

[19] G. E. Legge and J. M. Foley. Contrast masking in human vision. *J. Opt. Soc. Am.*, 70(12):1458–1471, Dec 1980.

[20] M. Nadenau. *Integration of human color vision models into high quality image compression*. PhD thesis, École Polytechnique Fédérale de Lausanne, 2000.

[21] A. Ninassi, O. Le Meur, P. Le Callet, and D. Barba. Which semi-local visual masking model for wavelet based image quality metric ? In *Proceedings of the 15th IEEE International Conference on Image Processing*, pages 1180 – 1183, San Diego, USA, Oct 2008.

[22] S.S. Gornale, R.R. Manza, V. Humbe, and K.V. Kale. Performance analysis of biorthogonal wavelet filters for lossy fingerprint image compression. *International journal of imaging science and engineering*, 1(1):16–20, Jan 2007.

[23] S. Grgic, K. Kers, and M. Grgic. Image compression using wavelets. In *Proc. IEEE Int. Symp. Industrial Electronics*, pages 99–104, Bled, Slovenia, 1999.

[24] N. Khalsa, G. G. Sarate, and D. T. Ingole. Evaluation of factors affecting the selection of mother wavelet to improve image compression of artificial & natural images. *International Journal on Computer Science and Technology*, 1(2):53–56, Dec 2010.

[25] E. Peli. Contrast sensitivity function and image discrimination. *Journal of the Optical Society of America A*, 18(2):283–193, 2001.

[26] P. Le Callet and D. Barba. A robust quality metric for color image quality assessment. In *International Conference on Image Processing (ICIP)*, volume 1, pages 437–440, Barcelona, Spain, Sep 2003. IEEE.

[27] H. R. Sheikh, Z. Wang, L. K. Cormack, and A. C. Bovik. LIVE image quality assessment database release 2. 18/7/11: `http://live.ece.utexas.edu/research/quality`, 2007.

[28] N. Ponomarenko, V. Lukin, A. Zelensky, K. Egiazarian, J. Astola, M. Carli, and F. Battisti. Tid2008 a database for evaluation of fullreference visual quality assessment metrics. *Advances of Modern Radioelectronics*, 10: 30–45, 2009.

[29] S. A. Ajagamelle, M. Pedersen, and G. Simone. Analysis of the difference of gaussians model in image difference metrics. In *5th European Conference on Colour in Graphics, Imaging, and Vision (CGIV)*, pages 489–496, Joensuu, Finland, Jun 2010. IS&T.

Author Biography

Marius Pedersen *is a researcher at the Norwegian Colour and Visual Computing Laboratory at Gjøvik University College, Norway. His work in centered on image quality assessment. He holds a BsC in Computer Engineering (2006) and a MiT in Media Technology (2007), both from Gjøvik University College. He received his PhD in Color Imaging in 2011 from the University of Oslo, Norway. He is currently the head of the Norwegian Colour and Visual Computing Laboratory.*